# Electronic structure of double-layer graphene tubules



doi: 10.1063/1.353358

# Electronic structure of double-layer graphene tubules

Riichiro Saito,[a),b)] G. Dresselhaus,[c)] and M. S. Dresselhaus[d)]
*Massachusetts Institute of Technology, Cambridge, Massachusetts 02139*

(Received 2 March 1992; accepted for publication 2 October 1992)

The electronic structure of coaxial, graphene double-layer tubules is predicted for various combinations of metallic and insulating constituent inner and outer monolayers, depending on the diameter and chirality of the tubule. For the examples chosen, some of the energy bands of the inner and outer tubules are coupled to each other by commensurate interlayer interactions. Nevertheless, because of symmetry, the energy bands of metallic monolayer tubules remain metallic even after interlayer interactions are considered. The possible implications of these results on molecular metal-insulator devices are discussed.

## I. INTRODUCTION

It has recently been postulated[1] and observed[2,3] that graphene tubules can be formed with diameters comparable to those of fullerenes, some tublules being a single monolayer in thickness. The electronic structure calculations of graphene monolayer tubules have predicted that both metallic and insulating monolayer tubules are possible, depending on the tubule diameter and its chirality.[4–9] However transmission electron microscope experiments do not usually show monolayer graphene tubules but rather multilayer (e.g., two, five, and seven) coaxial tubules in a fiber structure like the annual rings of a tree.[2] For these concentric tubules, some interlayer interactions may affect the energy bands near the Fermi level which are expected to have exotic electronic properties (e.g., ballistic transport and superconductivity), as are also observed in graphite intercalation compounds (GICs).[10] Though a coaxial multitubule structure is generally expected to be lattice mismatched for most inner and outer tubules, some interlayer correlations are expected. A general understanding of the electronic structure of multilayer tubules can be achieved by considering some simple cases. In this article we will present some calculated results for the electronic structure of graphene double-layer tubules, consisting of metal–metal, metal–insulator, and insulator-metal constituents. We conclude that almost all multilayer tubules are metallic if there is at least one metallic constituent monolayer tubule.

In Sec. II we summarize the results of monolayer tubules. In Sec. III the electronic structure for some simple examples of metallic-metallic and metallic-insulating double layers are shown. In Sec. IV we discuss the stability of the Fermi surface for metallic, chiral tubules with respect to the interlayer interaction and discuss the implication of this work on electronic devices.

## II. MONOLAYER TUBULES

First let us summarize the major results for monolayer graphene tubules.[5–7] The chirality and the radius of a monolayer graphene tubule are uniquely specified by the chiral vector $\mathbf{c}_h = n_1\mathbf{a}_1 + n_2\mathbf{a}_1 \equiv (n_1,n_2)$, where $n_1,n_2$ are integers and $\mathbf{a}_1,\mathbf{a}_2$ are the unit cell basis vectors of graphite. The chiral vector $\mathbf{c}_h$ is a circumferential lattice vector defined on a tubule surface, and $\mathbf{c}_h$ is perpendicular to the fiber axis. The fiber radius $r$ is defined by $r = |\mathbf{c}_h|/2\pi \equiv a\sqrt{n_1^2+n_1n_2+n_2^2}/2\pi$ where $a = 1.42\times\sqrt{3}$ Å is the lattice constant for graphite and the angle between $\mathbf{a}_1$ and $\mathbf{a}_2$ is 60°. The chiral angle of a tubule, $\theta = \arctan\{-\sqrt{3}n_2/(2n_1+n_2)\}$, is defined by the angle between $\mathbf{c}_h$ and $\mathbf{a}_1$. Since there are six definable angles for a tubule because of the hexagonal local structure, we select $|\theta| \leqslant 30°$ or $-n_1 \leqslant n_2 \leqslant n_1$, $(n_1 \geqslant 0)$.

The one-dimensional (1D) energy bands of a monolayer graphene tubule are obtained from the two-dimensional (2D) energy dispersion relations for the $\pi$ bands of graphite by eliminating one of the two components of the wave vector $k$ according to the periodic boundary condition in the circumferential direction,

$$\mathbf{c}_h \cdot k = 2\pi m, \tag{1}$$

where $m$ is an integer.[5] If the $k$ value at the energy degenerate points of the 2D graphite $\pi$ bands satisfies this boundary condition for an $m$ value, the corresponding 1D energy band is degenerate at the Fermi level and the fiber is metallic with a finite density of states at $E = E_F$. The condition for a monolayer graphene tubule to be metallic is expressed by[6–8]

$$2n_1 + n_2 = 3q, \tag{2}$$

where $q$ in an integer.

## III. DOUBLE-LAYER TUBULES

Using these results for the graphene monolayer tubules, we design some graphene double layers in which we simply select two chiral vectors, $(p,q)$ and $(r,s)$, for the inner and outer tubules, respectively. Strictly speaking we should define some phase parameter which specifies the relative positions of the two chiral vectors. For simplicity, we do not consider this general situation, but instead we

[a)]Permanent address: University of Electro-Communications, Chofu, 182 Tokyo, Japan.
[b)]Department of Physics.
[c)]Francis Bitter National Magnet Laboratory.
[d)]Department of Electrical Engineering and Computer Sciences and Department of Physics.

 0021-8979/93/020494-07$06.00  

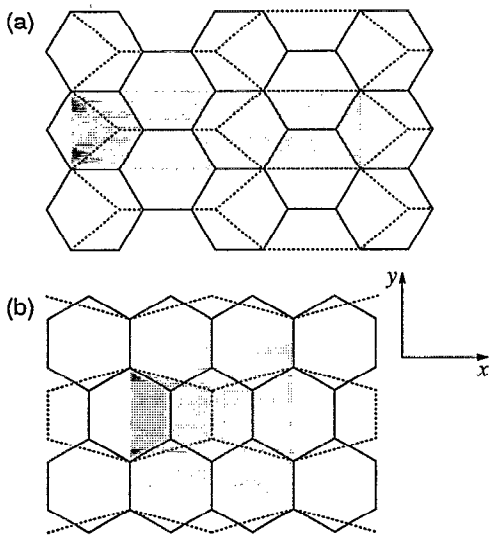


FIG. 1. Unit cells of double-layer tubules (shaded area) for (a) (5,5)-(10,10) and (b) (9,0)-(18,0) tubule pairs, respectively. The inner-tubule lattice structure (dotted line) is projected on the outer one (solid line).

adjust the relative orientation of the tubules so as to match the carbon site locations on the inner and outer tubules as best we can for each pair of coaxial tubules. The differences in the radii of the two tubules are selected to be close to the layer–layer separation of turbostatic graphite, $c_0=3.44$ Å.[11]

### A. Commensurate metallic–metallic double-layer tubules

We first consider the two best-matched, double-layer tubules, and these consist of two tubule pairs, (5,5)-(10,10) and (9,0)-(18,0). All four monolayer constituent tubules are known to be metallic from Eq. (2). The inner monolayer tubules, (5,5) and (9,0), are both considered to be minimum diameter graphene tubules, since they can be generated from a hemisphere of $C_{60}$ whose radius (3.42 Å) is close to $c_0$, the $c$-axis lattice constant of graphite.[1] Thus the differences in radii between these monolayer tubules and their double-size tubules in both cases are close to $c_0$, too. Actually the differences in radius, as defined above, are 3.39 and 3.52 Å for the (5,5)-(10,10) and (9,0)-(18,0) fibers pairs, respectively. It should be noted that there is a significant difference in the layer separation $c_0$ between single crystal graphite with correlated layers (3.35 Å) and turbostratic graphite with uncorrelated layers (3.44 Å).

In Fig. 1 we show unit cells (shaded area) for the double-layer tubules defined by (a) (5,5)-(10,10) and (b) (9,0)-(18,0), respectively. In order to see the relative positions of atoms for the inner and outer tubules, the inner-tubule lattice structure (dashed lines) is projected on the outer one (solid lines) through enlargement by a factor of 2 in the circumferential direction ($x$) while not enlarging the structure along the fiber axis direction ($y$). As seen in the figure, one of two carbon atoms in an inner graphene tubule can interact with one of four carbon atoms in the outer tubule. This stacking is similar to $AB$ stacking in graphite.[10] We adopt the interlayer interaction of three-dimensional (3D) graphite denoted by $\gamma_1$ (Ref. 10) for carbon atoms on adjacent tubules, and do not consider any other interactions for simplicity. Actually we would expect the interlayer interaction to be less for the tubules in comparison to graphite, since the interlayer separation is greater for the tubules and some hybridization due to the curvature occurs.

The energy bands are here calculated by a simple tight binding model for $\pi$ bands in which we consider only nearest-neighbor interactions within a graphene layer, and use the same values for the intralayer and interlayer interactions as for 3D graphite, $\gamma_0=3.13$ and $\gamma_1=0.35$ eV, respectively. We solve the 2D energy band calculation for twelve carbon atoms in each unit cell by substituting the discrete $k_x$ values for the periodic boundary conditions for each tubule to obtain 1D energy bands. Even for such a simple model, we can predict the energy bands near the Fermi energy quite well, as is also the case for GICs.[12,13] Since the energy dispersion relations have electron-hole symmetry, we always have $-E$ eigenvalues whenever we have $+E$ eigenvalues. Thus we show in the figures of this article explicitly only $E>0$ (antibonding energy bands) for simplicity. Since the Fermi energy for these bands is located at $E=0$, the energy gap is defined as twice the minimum energy for energy bands having a minimum for $E>0$ and the system is metallic if the minimum energy is at $E=0$.

In Fig. 2 we show the energy dispersion relations of pairs of tubules for (5,5)-(10,10) [for (a) and (b)] and (9,0)-(18,0) [for (c) and (d)]. The interlayer interaction $\gamma_1$ as described above is introduced in Figs. 2(a) and 2(c). Also shown in Figs. 2(b) and 2(d) for comparison are the corresponding energy bands when $\gamma_1$ is set equal to zero. When the interlayer interaction between the double layers is not considered, the $E(k)$ relations are just the overlay of the energy dispersion relations of the unperturbed inner and outer tubules as expected. For example, the energy dispersion, $E_m^{(N,N)}(k)$ for $(N,N)$ armchair fibers can be expressed as[5]

$$E_m^{(N,N)}(k)=\pm\gamma_0\left[1\pm 4\cos\left(\frac{m\pi}{N}\right)\cos\left(\frac{ka}{2}\right)+4\cos^2\left(\frac{ka}{2}\right)\right]^{1/2},$$

for

$$\left(-\frac{\pi}{a}<k<\frac{\pi}{a}\right),\quad (m=0,\ldots,N-1), \tag{3}$$

where there are four different branches given by this equation. Setting $N_{\text{in}}=5$ and $N_{\text{out}}=10$ for inner and outer constituents of the (5,5)-(10,10) fiber, we can see thirty (eleven inequivalent) energy dispersion relations for $E>0$ as shown in Fig. 2(b) in which the $m$ values for outer $[m_{\text{out}},\ldots]$ and inner $(m_{\text{in}},\ldots)$ tubules and the $\pm$ signs correspond, respectively, to the folded and unfolded energy bands appearing in $\{1\pm\ldots\}$ of Eq. (3). The folded and unfolded energy bands have different symmetries and therefore can cross without interacting. In the case of

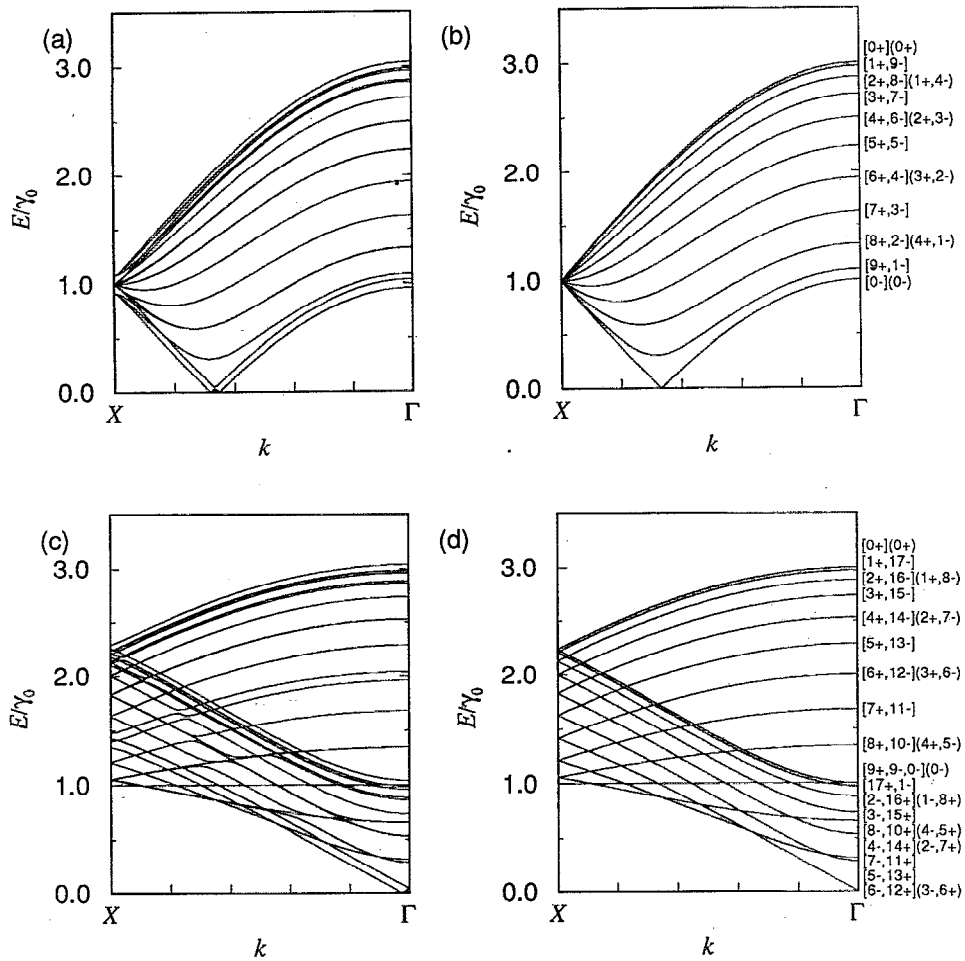


FIG. 2. Energy dispersion relation for the tubule pairs (5,5)-(10,10) [(a) and (b)] and (9,0)-(18,0) [(c) and (d)] in which the interlayer interaction $\gamma_1$ is introduced in (a) and (c) and not in (b) and (d) for comparison. The numbers with [...] and (...) reflect $m$ values for $E_m(k)$ for the outer and inner tubules, respectively, and the $\pm$ signs correspond to the folded and unfolded energy bands.

$\gamma_1=0$, the integers $m_{\text{in}}$ and $m_{\text{out}}$ are good quantum numbers for specifying energy bands. The degeneracies in the dispersion relations come from two sources: (1) the $m=p$ and $m=(N-p)(p=1,...,N-1)$ energy bands are degenerate for each of the tubules, and (2) the energy bands with $m_{\text{in}}=p$ and $m_{\text{out}}=2p$ are degenerate for any $p(p=0,...,N_{\text{in}}-1)$ for the $(N,N)$-$(2N,2N)$ tubules.

When the interlayer interaction $\gamma_1$ is switched on, some energy dispersion relations are split by the interlayer interaction. Since the interlayer interaction for the (5,5)-(10,10) tubules has the full point group symmetry of the group $D_{5d}$ (and $A_{1g}$ symmetry for the inner tubule) as shown in Fig. 1(a), $m_{\text{in}}$ is a good quantum number for the twelve carbon atoms in the unit cell. We then solve the $12\times12$ Hamiltonian for $m_{\text{in}}=0,...,4$ to obtain sixty energy bands (thirty for $E>0$). The energy bands with different $m_{\text{in}}$ can cross each other. The degeneracy of energy bands for all $k$ points, which is 2 or 4 when $\gamma_1=0$, becomes 1 or 2 because of the $D_{5d}$ symmetry, though this is difficult to resolve from Fig. 2(a) except for certain energy bands with stronger interactions.

For the (5,5)-(10,10) tubules, the energy bands at the $X$ points $(k\pm\pi/a)$ are degenerate at $E=0$ for any $m_{\text{in}}$ when $\gamma_1=0$ [Fig. 2(b)]. These levels are generally split into three levels: $E=\gamma_0$, $\gamma_0\pm\gamma_1/\sqrt{2}$ as shown in Fig. 2(a), when $\gamma_1$ is introduced. More precisely, the determinant of the $12\times12$ Hamiltonian matrix (which does not depend on $m_{\text{in}}$) at the $X$ point for a (5,5)-(10,10) tubule pair, can be factored as follows:

$$\det(\mathscr{H}-EI)=(e-1)^3(e+1)^3(e^3-e^2-e-g_1^2e+1)\times(e^3+e^2-e-g_1^2e-1)=0, \tag{4}$$

in which $e=E/\gamma_0$ and $g_1=\gamma_1/\gamma_0$. Solving Eq. (4) assuming that $g_1$ is small, we get the eigenvalues $e=\pm1$ which are each triply degenerate for each $m_{\text{in}}$, and $e\sim\pm(1-g_1^2/4)$, $\pm(1\pm g_1/\sqrt{2})$. Since $g_1=0.11$ in the present case, the $g_1^2/4$ term can be neglected compared with 1 and thus we will obtain approximately the two branches $E=\pm\gamma_0$ and the four branches $E=\pm(\gamma_0\pm\gamma_1/\sqrt{2})$.

For general $k$ points, the splitting of the energy bands for the (5,5)-(10,10) tubules is significant only for energy bands with $m=0$ while the splitting is seen for all energy bands near the $X$ points as shown in Fig. 2(a). This can be explained by the symmetry of the interlayer interaction and that of the unperturbed wave function of the inner and

outer tubules when we assume the interlayer interaction to be a perturbation between the degenerate energy bands. The matrix elements of the interlayer interaction between energy bands of the inner and outer tubule becomes large when $m_{in}=m_{out}$ for any combination of the signs, as shown in Appendix A. Using the fact that the energy bands with $m_{in}=p$ and $m_{out}=2p$ are degenerate, we conclude that only $m=0$ energy bands of tubule pairs interact with each other within first order perturbation theory. The remaining splittings of the energy bands predicted by group theory are a higher order perturbation between nondegenerate energy bands and the splitting is generally small.

It is important to note that the (5,5)-(10,10) concentric armchair tubules are metallic even when the interlayer interaction is considered. This is simply because the wave functions of the valence and conduction bands which are degenerate at $E=0$, have the same components of carbon atoms on the inner (or outer) tubules with different symmetries. Thus the coupling for the interlayer interaction vanishes at $E=0$. Thus the degenerate bands at $E=0$ are not split by the interlayer interaction, though the energy bands with $m=0$ are split. This result is similar to the fact that energy bands for the second stage GICs have a zero energy gap though the $\pi$ band in general is split by the interlayer interaction.[12]

For the (9,0)-(18,0) concentric zigzag tubules, the situation is similar to the case of the (5,5)-(10,10) armchair tubules. The energy dispersion relations for the $(N,0)$ tubules without any interlayer interaction are also specified[5] by a quantum number $m$ as

$$E_m^{(N,0)}(k)=\pm\gamma_0\left[1\pm 4\cos\left(\frac{\sqrt{3}ka}{2}\right)\cos\left(\frac{m\pi}{N}\right)+4\cos^2\left(\frac{m\pi}{N}\right)\right]^{1/2},$$

for

$$\left(-\frac{\pi}{\sqrt{3}a}<k<\frac{\pi}{\sqrt{3}a}\right),\quad (m=0,\ldots,N-1), \tag{5}$$

where there are four branches. In Fig. 2(d) we list the $m$ values and $\pm$ sign for the folded and unfolded energy bands appearing in $[1\pm\ldots]$ for the (9,0)-(18,0) tubules without any interlayer interactions. When the interlayer interaction is turned on, the degenerate energy bands with $m_{in},m_{out}=0,6$ are split, for the same reason as that in the case of the (5,5)-(10,10) tubule pair. Similarly we can see in Fig. 2(c) anticrossings of the energy bands at some $k$ points for the degenerate energy bands of the inner and outer tubules with $m_{in}=m_{out}$. For general $k$ points all four degenerate energy bands split up into a degeneracy of 2 by the interlayer interaction, since the interlayer interaction has the full point group symmetry of the group $D_{9d}$.

Referring to Fig. 2(c), at the Fermi level, a zero-energy gap appears near the $\Gamma$ point for the interacting (9,0)-(18,0) tubule pair. Thus the two cases shown in Fig. 2 for double tubules consisting of two-metallic graphene tubules are predicted to be metallic.

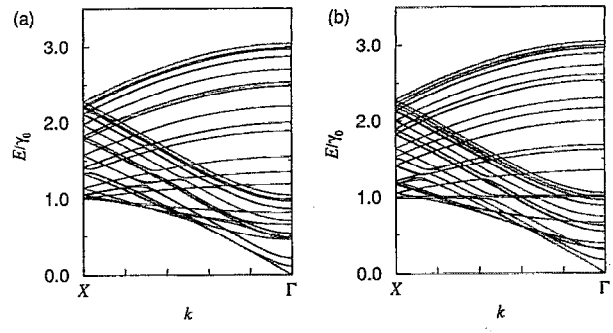


FIG. 3. Energy dispersion relations for (a) (9,0)-(17,0) (metallic-insulating) and (b) (10,0)-(18,0) (insulating-metallic) tubules.

### B. Incommensurate metallic–insulating double tubules

Next we consider double tubules whose diameter ratio for outer to inner tubules is not an integer. Usually the word "incommensurate" is used when the ratio of two different lattice constants is irrational. Since the number $m$ for the periodicity in the circumferential direction is finite, the lattice structure is always commensurate by this definition. Here "incommensurate" means that $N_{in}$ and $N_{out}$ have no large common factor. For most large diameter tubules two adjacent tubules are generally expected to be incommensurate. Of special interest are the cases of semiconductor-metallic or metallic-semiconductor tubules, since we can consider them as a molecular conductive wire covered by an insulator or as a molecular capacitor in a memory device, respectively.

Here we consider the tubule pairs (9,0)-(17,0) and (10,0)-(18,0) as examples of metal-insulator and insulator-metal graphene tubules referring to Eq. (1). For both tubule pairs the differences in radii are 3.132 Å (8.6% smaller than $c_0$). Though the lattice structure is not correlated because of the large difference in radius, we consider a local lattice matching between the inner and outer tubules to occur, just as we considered for the case of the (9,0)–(18,0) [see Fig. 1(b)], where the carbon atoms of the inner and outer tubules have the same $y$ coordinates in the direction of the fiber axis ($y$ axis). The interlayer interaction is considered only for atoms with the same $y$ coordinate whose difference in atom positions in the circumferential direction ($x$ axis), $\Delta x$, is smaller than $a/3$, when the lattice of the inner tubule is projected onto that of the outer tubule. Though the minimum distance for two carbon atoms for different $y$ coordinates $a/2\sqrt{3}$ is less than $a/3$, the interlayer interactions between these atoms are not considered, consistent with our treatment in the previous section [Fig. 1(b)]. The magnitude of the interlayer interaction is taken as $\gamma_1\exp(-|\Delta x|/a)$. The choice of the damping factor $a$ in the exponential decay is motivated by the situation in graphite where the interlayer interaction for carbon atoms separated by two layers quickly decreases with increasing distance, thereby justifying this choice of the damping factor.

In Figs. 3(a) and 3(b), the energy dispersion relations are shown for (9,0)-(17,0) and (10,0)-(18,0) tubules

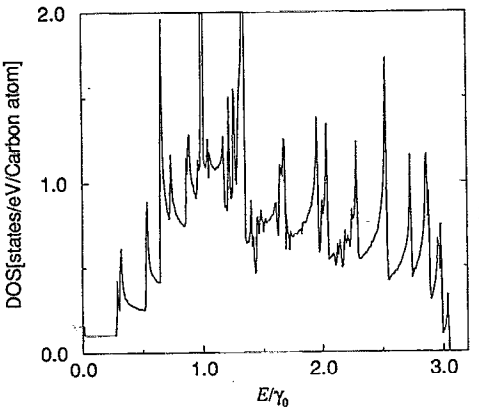


FIG. 4. Density of states of a (9,0)-(18,0) tubule pair.

pairs, respectively. Since there is no common rotational symmetry operation between these double-layer tubules, all energy bands are nondegenerate when $\gamma_1 \neq 0$. The anticrossing of the energy bands and the splitting of the energy bands for the inner and outer tubules can be seen in the figure. These effects are similar to those of commensurate tubules. In Fig. 3(a) and 3(b) the energy bands have no energy gap at the Fermi energy. The energy bands near the Fermi energy originate from the metallic tubules (9,0) and (18,0), associated with the (9,0)-(17,0) and the (10,0)-(18,0) tubule pairs, respectively. Since these energy bands are not degenerate with those from the other tubules which are insulating, the interlayer interaction does not act to open the energy gap, Thus it is concluded that the combination of metallic and insulating graphene tubules retain the basic electronic properties of each constituent graphene monolayer tubule, even though the detailed energy dispersion relations are affected by the interlayer interaction.

Finally we show the density of states for the (9,0)-(18,0) metal-metal tubule pair in Fig. 4. The density of states of double layers is very singular, reflecting 1D van Hove singularities at the many anticrossings of energy bands, as shown in Fig. 2(c) due to the interlayer interaction. The broadened density of states of a double-layer tubule may perhaps be observed by scanning tunneling spectroscopy (STS) which is widely used for observing the local electronic structure of semiconductor surfaces. In STS experiments we can distinguish whether or not the observed fiber is metallic by measuring $\partial I/\partial V$ without applying bias voltage $V$. By further changing $V$, we will get information on the density of states of the tubule, though the electric current is a function of the position of the tip. If we can measure the energies where singularities in the density of states occur with sufficient accuracy, we can then estimate the chiral vectors that we use for specifying the outermost tubules. Though getting similar information for the inner tubules will be more difficult, we can estimate the radius and chirality by observing the difference of the radii between the inner and outer tubules.

When an alkali-metal atom dopant is introduced into these fibers and charge transfer from an alkali-metal atom to graphite occurs, a high density of states at the Fermi level could be expected. In comparison to the case of 2D graphite for which a logarithmic singularity in the density of states appears at about 3 eV ($E=\gamma_0$) above the Fermi energy, the 1D van Hove singularities appear at a much lower energy region near the Fermi level. Thus in the region where the Fermi energy can be changed by alkali-metal doping, we can adjust the Fermi energy to coincide with a singular energy point in the density of states. Though it is difficult to change the charge transfer value of an alkali-metal atom, the singular energy position of the density of states can be changed by changing the fiber diameter and the chirality. Thus a more exotic behavior of the transport properties (e.g., ballistic transport) in such graphene tubules would be expected than is seen in GICs. Further the high density of states at the Fermi level for doped tubules might be favorable for the occurrence of superconductivity as is, for example, observed in the first stage GIC $C_8K$.[10]

## IV. DISCUSSION

Based on some of the simple examples shown in the previous section, we now discuss the case of multilayer tubules consisting of at least one metallic tubule. We showed in the previous section that the metallic energy bands are generally stable under the interlayer interaction between two graphene tubules.

For a general fullerene-based fiber, a chiral structure is generally expected, especially for large diameter fibers, because of the large number of chiral vectors that are possible with increasing $\mathbf{c}_h$. In a general two-layered chiral fiber, the two graphene tubules are expected to be incommensurate and they have only $2\pi$ rotational symmetry along the chiral vectors which are both perpendicular to the fiber axis. Thus the energy bands of the inner tubule are not degenerate with those of the outer tubule. When we consider a metallic graphene tubule, the energy bands of the bonding and antibonding $\pi$ bands are degenerate at $E=0$ and their symmetries are different from each other. To open an energy gap at the degenerate points by the interlayer interaction, it is necessary to have nonvanishing matrix elements between the two energy bands. Since the interlayer interaction couples the energy bands for inner and outer tubules, the matrix elements should contain terms in at least second order in the perturbation, $g_1^2$. Therefore the lifting of the degeneracy is generally small even if there are nonvanishing matrix elements between the two degenerate energy bands.

Further when we expand the incommensurate, interlayer interaction in the direction of the chiral vector in a Fourier series, the matrix element, calculated using Bloch functions for the inner and outer tubules, becomes small in almost all cases through a cancellation of the phase factors arising from the Bloch functions and the interaction Hamiltonian. Thus in general cases it is concluded that no energy gap will open for a metallic tubule in a general incommensurate chiral graphene tubule pair. For the same reason, insulator-insulator tubules do not become metallic by introducing only interlayer interaction. If the energy level position of carbon $2p_z$ is different for inner and outer

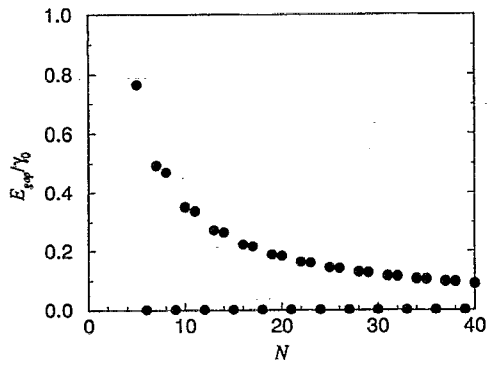


FIG. 5. Energy gap of $(N,0)$ zigzag tubules as a function of $N$.

tubules, a semimetallic nature of the Fermi surface will be expected. In the case of the higher stage GICs, an inhomogeneous $c$ axis charge distribution of the carriers donated from alkali-metal layers causes a different potential energy for carbon 2 $p_z$ orbitals in inequivalent layers.[10] However in this case all layers are still metallic since there are no hole bands for the occupied $\pi$ bands.

Metal-insulator-semiconductor devices can in principle be designed based on these carbon tubules. Since the metallic and insulating nature of the constituent monolayer tubules is expected to be preserved for triple layer graphene tubules, we can select a set of chiral graphene tubules whose differences in radii are close to $c_0$. From the inner to outer tubules, there are two interesting possibilities for the molecular design of devices: metal-insulator-semiconductor and semicon-ductor-insulator-metal tubules. For the first case, if we can put alkali-metal atoms along the axis of the tubules, we can make a metallic tubule covered by an insulating one, and in the outermost tubules we can prepare narrow gap semiconductors since the energy gap $E_{gap}$ decreases as $\sim 1/N$ with increasing $N$ for $(N,0)$ tubules. The dependence of $E_{gap}$ on $N$ is obtained analytically from Eq. (5) by putting $k=0$ and by selecting the $m$ values corresponding to the minimum energy bands for $E>0$ to yield,

$$E_{gap}=2\gamma_0\left[1-2\cos\left(\frac{(N+1)/3\pi}{N}\right)\right], \tag{6}$$

where the symbol $[Q]$ represent the Gauss' symbol, that is, the maximum integer which is not larger than $Q$. If $N$ is not a multiple of 3, the energy gap for a given $N$ has a finite value. Values for $E_{gap}$ monotonically decrease with increasing $N$ as shown in Fig. 5. For the semiconductor–insulator–metal case, some doping should be done to increase the conductivity of the innermost semiconductor tubule. Because of the cylindrical geometry of these structures, the electric field for controlling the device will be larger than for planar devices and thus a shorter switching time would be expected.

Since the electronic structure has uniaxial symmetry, it will be of interest to consider the magnetic response of the transport properties for magnetic fields in the direction of the fiber axis. Furthermore even for double-layer tubules, there is the possibility of changing the electronic structure by changing the relative positions of the inner and outer tubules, which control the amount of lattice matching.

For the thickening of fullerene tubules, experimental results for vapor grown carbon fibers show that crystal growth of fullerene fibers takes place by accumulating carbon species at pentagonal sites within the nucleating cap.[14] In this sense we can make a super-tubule structure like a semiconductor superlattice structure, if we simply specify an innermost tubule which is grown by a nucleation cap. If the thickness, diameter, and chirality of such carbon fibers can be controlled during the growth process, new carbon physics will result and perhaps lead to the application of these structures to electronic devices.

In summary we calculated the electronic structure of some double-layer graphene tubules and we show that because of symmetry reasons, the interlayer interaction between the layers does not affect the metallic nature of the constituent. The application of double- and triple-layer tubules for devices is discussed.

## ACKNOWLEDGMENTS

The authors would like to thank Dr. M. Fujita and Professor M. Endo for valuable discussions. One of the authors (R.S.) has carried out this work while a visiting scientist at MIT as Overseas Research Scholars of the Ministry of Education, Science, and Culture of Japan. We gratefully acknowledge National Science Foundation grant No. DMR88-19896 for support of this research.

## APPENDIX: THE MATRIX ELEMENT OF THE INTERLAYER INTERACTION

Here we consider matrix elements for $(N,N)$-$(2N,2N)$ and $(N,0)$-$(2N,0)$ tubule pairs. A 1D Bloch function, $\Psi_j^m(k,y)$, for a $2p_z$ orbital, $\phi_j$, $(j=1,...,12)$ in the unit cell of the tubule geometry (see Fig. 1) can be expressed by

$$\Psi_j^m(k,y)=\frac{1}{\sqrt{N}}\sum_Y e^{ikY}\sum_{l=1}^{N_x} e^{im\varphi_l}\phi_j(\varphi-\varphi_l, y-Y),$$
$$(m=0,...,N_x-1), \tag{A1}$$

where $N_x$ is the number denoting the periodicity in the circumferential direction and $\varphi_l=2\pi l/N_x$ is an angle in the cylindrical coordinate system, and $l$ is an integer between 1 and $N_x$. Then a matrix element of the interlayer interaction, $\mathscr{H}_{int}$, which couples the Bloch function of an inner tubule with that of an outer tubule, is obtained by

$$\langle\Psi_{j'}^{m_{out}}(k',y)|\mathscr{H}_{int}|\Psi_j^{m_{in}}(k,y)\rangle$$
$$=\frac{1}{N}\sum_{Y,Y'} e^{-i(k'Y'-kY)}\sum_{l'=1}^{N_x^{out}}\sum_{l=1}^{N_x^{in}} e^{i(-m_{out}\varphi_{l'}+m_{in}\varphi_l)}$$
$$\times\langle\varphi_{j'}(\varphi-\varphi_{l'}, y-Y')|\mathscr{H}_{int}|\phi_j(\varphi-\varphi_l, y-Y)\rangle. \tag{A2}$$

In the best matched lattice structure as shown in Fig. 1, we need to consider the matrix element of atomic orbitals for

some combination of the $j$ and $j'$th carbon atoms which satisfy $\varphi_{l'}=\varphi_l$ and $Y'=Y$. For such a set of $j$ and $j'$, the matrix elements become

$$\langle \Psi_{j'}^{m_{\text{out}}}(k',y)\,|\,\mathscr{H}_{\text{int}}\,|\,\Psi_{j}^{m_{\text{in}}}(k,y)\rangle$$

$$=\frac{1}{N}\sum_{Y} e^{-i(k'-k)Y}\sum_{l=1}^{N_x^{\text{in}}} e^{i(-m_{\text{out}}+m_{\text{in}})\varphi_l}\gamma_1$$

$$=\delta_{k,k'}\delta_{m_{\text{out}},m_{\text{in}}}\gamma_1. \tag{A3}$$

Thus when $m_{\text{out}}=m_{\text{in}}$, $(m_{\text{in}}=0,\ldots,N_x^{\text{in}}-1)$ the matrix element between Bloch orbitals of carbon atoms for inner and outer tubules is large for any $k$.


[1] M. S. Dresselhaus, G. Dresselhaus, and R. Saito, Phys. Rev. B **45**, 6234 (1992).

[2] S. Iijima, Nature **354**, 56 (1991).

[3] M. Endo, H. Fujiwara, and E. Fukunaga, Meeting of the Japanese Physical Society (1991), p. 34; 2nd $C_{60}$ Symposium in Japan, Japanese Chemical Society, 1992, p. 101.

[4] J. W. Mintmire, B. I. Dunlap, and C. T. White, Phys. Rev. Lett. **68**, 631 (1992).

[5] R. Saito, M. Fujita, G. Dresselhaus, and M. S. Dresselhaus, Phys. Rev. B **46**, 1804 (1992).

[6] R. Saito, M. Fujita, G. Dresselhaus, and M. S. Dresselhaus, in *Electrical, Optical, and Magnetic Properties of Organic Solid State Materials*, MRS Symposia Proceedings, Boston, edited by L. Y. Chiang, A. F. Garito, and D. J. Sandman (Materials Research Society, Pittsburgh, PA, 1992), Vol. 247, p. 333.

[7] R. Saito, M. Fujita, G. Dresselhaus, and M. S. Dresselhaus, Appl. Phys. Lett. **60**, 2204 (1992).

[8] N. Hamada, S. Sawada, and A. Oshiyama, Phys. Rev. Lett. **68**, 1579 (1992).

[9] K. Tanaka, K. Okahara, M. Okada, and T. Yamabe, Chem. Phys. Lett. **191**, 469 (1992).

[10] M. S. Dresselhaus and G. Dresselhaus, Adv. Phys. **30**, 139 (1981).

[11] M. S. Dresselhaus, G. Dresselhaus, K. Sugihara, I. L. Spain, and H. A. Goldberg, in *Graphite Fibers and Filaments* (Springer-Berlin, 1988), Vol. 5.

[12] J. Blinowski and C. Rigaux, J. Phys. (Paris) **61**, 667 (1980).

[13] J. Blinowski and C. Rigaux, J. Phys. (Paris) **45**, 545 (1984).

[14] M. Endo and H. W. Kroto, J. Phys. Chem. **96**, 6941 (1992); R. Saito, G. Dresselhaus, and M. S. Dresselhaus, Chem. Phys. Lett. **195**, 537 (1992).